

Impurity effects on resonant Andreev reflection in a finite-sized carbon nanotube system

Hui Pan, Tsung-Han Lin, and Dapeng Yu

State Key Laboratory for Mesoscopic Physics and Department of Physics, Peking University, Beijing 100871, People's Republic of China

(Received 22 June 2004; published 9 December 2004)

The impurity effects on resonant Andreev reflection through a normal-metal/carbon-nanotube/superconductor system are studied theoretically. The Andreev reflection current versus gate voltage clearly shows that the impurity can break the electron-hole symmetry in nanotubes, and the symmetry broken depends distinctly on the impurity strength. The length of the armchair nanotube can cause the on-resonance and off-resonance behavior of the Andreev reflection. For the on-resonance case, the impurity narrows the distribution of the Andreev reflection probability and decreases the current, while for the off-resonance case, the impurity enhances the Andreev reflection probability and increases the current.

DOI: 10.1103/PhysRevB.70.245412

PACS number(s): 73.23.Ad, 72.80.Rj, 73.63.Fg

Carbon nanotubes have been the subject of an increasing number of experimental and theoretical studies due to their quasi-one-dimensional structure and unique electronic property.¹ The perfect carbon nanotube is predicted to be either metallic or semiconducting sensitively depending on its diameter and chirality, which is uniquely determined by the chiral vector (n, m) , where n and m are integers.¹⁻⁴ Experimental and theoretical studies have indicated that the electronic and transport properties of carbon nanotubes can be substantially modified by point defects such as the substitutional impurities.⁵⁻¹¹ Recent interests concentrate on the electron transport through a hybrid nanotube system. Experiments about some hybrid systems including nanotube-based magnetic tunnel junctions¹² and superconducting junctions^{13,14} have been successfully fabricated. The electrical transport about the carbon nanotube quantum dot in the Kondo regime coupled to a normal and a superconductor has also been reported.¹⁵ The theoretical investigation of transport properties of these hybrid nanotube devices is of great importance, not only for their basic scientific interest, but also aiming at the design of novel nanodevices.

The resonant Andreev reflections in the superconductor/carbon-nanotube devices has been theoretically studied.¹⁶ The proximity effect in superconductor/carbon-nanotube/superconductor (S/CNT/S) tunnel junctions has also been studied theoretically.^{17,18} Since carbon nanotubes are not strictly one-dimensional (1D) materials but are quasi-1D ones, it is expected that the impurity has unique effects on the resonant Andreev tunneling. How does the impurity influence the Andreev reflection of the CNT system? Does the impurity simply suppress the Andreev reflection probability and current? In order to answer these questions, in this paper, the impurity effects on the resonant Andreev reflection in the hybrid normal-metal/carbon-nanotube/superconductor (N/CNT/S) system are theoretically studied. In such a system, the specific molecular orbital plays an important role. By combing standard nonequilibrium Green's function (NGF) techniques¹⁹⁻²¹ with a tight-binding model,^{22,23} we have analyzed the quantum transport properties of the N/CNT/S system with an impurity. The Andreev reflection through the finite-sized carbon nanotube depends on the impurity strength and the tube length. The tube length causes the on-

resonance and off-resonance behavior of Andreev reflection. Since the impurity changes the energy structure of the CNT, it has a great influence on the Andreev reflection of the system. The dependence of the Andreev reflection current on the gate voltage is also studied.

We assume that the system N/CNT/S under consideration is described by the following Hamiltonian:

$$H = H_L + H_R + H_{CNT} + H_T, \quad (1)$$

where

$$\begin{aligned} H_L &= \sum_{k,\sigma} (\epsilon_{L,k}^0 - eV_L) a_{L,k\sigma}^\dagger a_{L,k\sigma}, \\ H_R &= \sum_{p,\sigma} \epsilon_{R,p}^0 a_{R,p\sigma}^\dagger a_{R,p\sigma} + \sum_p [\Delta^* a_{R,p\downarrow} a_{R,-p\uparrow} + \Delta a_{R,-p\uparrow}^\dagger a_{R,p\downarrow}^\dagger], \\ H_{CNT} &= \sum_{i,\sigma} (\epsilon_i^0 - eV_g) c_{i\sigma}^\dagger c_{i\sigma}, \\ H_T &= \sum_{k,\sigma,i} [t_L a_{L,k\sigma}^\dagger c_{i\sigma} + \text{H.c.}] + \sum_{p,\sigma,i} [t_R e^{iev_R\tau} a_{R,p\sigma}^\dagger c_{i\sigma} + \text{H.c.}], \end{aligned} \quad (2)$$

where H_L describes the noninteracting electrons in the left normal-metal lead, $a_{L,k\sigma}^\dagger$ ($a_{L,k\sigma}$) are the creation (annihilation) operators of the electron in the left lead, and v_L is the voltage of the left lead. H_R describe the right superconducting lead with the energy gap Δ . H_{CNT} is the Hamiltonian of the central CNT with multiple discrete energy levels ϵ_i^0 . It is noted that the electron-electron interaction is important and results in the Luttinger liquid behavior in nanotubes.^{24,25} However, some transport properties in nanotubes can be well explained by using a single-electron model despite the possible important electron-electron interaction effect.^{13,14,16,17} One can obtain a qualitative understanding of the experimental results observed from a single-electron picture of electron transport in the CNT.^{13,14,16,17} The reason may be that a single-electron description is appropriate when the bias voltage and the temperature are much lower than the energy-level spacing of the experimental sample. Based upon this consideration, in this paper, the single-electron model is used. v_g is the gate volt-

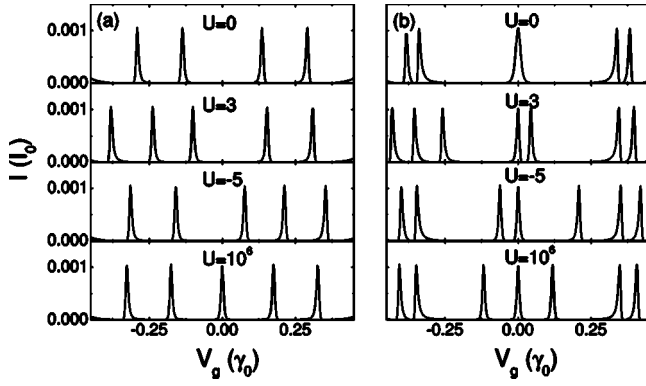


FIG. 1. Andreev reflection current I_A vs the gate voltage for the (6,6) nanotube of length (a) $L=6$ and (b) $L=7$ with different impurity strength U . Here, $V=0.5\Delta$, and $\Gamma=0.01\gamma_0$.

age which controls the energy levels in the CNT. H_T denotes the tunneling part of the Hamiltonian, and $t_{L,R}$ are the hopping matrix. ϵ_i^0 can be obtained from the Hamiltonian of the nanotube with an impurity, which is described by the tight-binding model with one π electron per atom as

$$H_{tube} = \sum_{\langle i,j \rangle, \sigma} [-\gamma_0 C_{i\sigma}^\dagger C_{j\sigma} + \text{H.c.}] + UC_0^\dagger C_0, \quad (3)$$

where the sum in i, j is restricted to nearest-neighbor atoms, and the bond potential $\gamma_0=2.75$ eV, which is used as the energy unit in the following calculations. This model is known to give a reasonable, qualitative description of the electronic and transport properties of carbon nanotubes.^{22,23} We focus on metallic armchair nanotubes of finite length L . For armchair nanotubes, L is measured in terms of unit cell. A unit cell is the repeat unit along the armchair tube consisting of two carbon rings. The pointlike defect is defined by setting site energy equal to U at one of the sites of the unit cell, and various strengths represent typical substitutional impurities or vacancy.¹⁰ This perturbation can represent an impurity or a point vacancy. For example, the strength $U=3, -5$, and 10^6 can simulate the substitutional boron, nitrogen, and vacancy, respectively, according to former tight-binding and *ab initio* calculations.^{10,11} Similar to the methods used before to deal with the central part,¹⁷ H_{tube} can be numerically diagonalized to obtain ϵ_i^0 , the discrete energy levels for the isolated nanotube with the impurity. Then the probability and current of Andreev reflection can be calculated from standard NGF techniques.

It is convenient to introduce the 2×2 Nambu representation in which the Green's function can be expressed by

$$\begin{aligned} \mathbf{G}^{r,a}(\tau, \tau') & \\ &= \mp i\theta(\tau \mp \tau') \sum_{ij} \begin{pmatrix} \langle c_{i\uparrow}(\tau), c_{j\uparrow}^\dagger(\tau') \rangle & \langle c_{i\uparrow}(\tau), c_{j\downarrow}(\tau') \rangle \\ \langle c_{i\downarrow}^\dagger(\tau), c_{j\uparrow}^\dagger(\tau') \rangle & \langle c_{i\downarrow}^\dagger(\tau), c_{j\downarrow}(\tau') \rangle \end{pmatrix}. \end{aligned} \quad (4)$$

Without couplings to the leads, the retarded Green's function of the isolated CNT is calculated as^{17,21}

$$\begin{aligned} g^r(\tau, \tau') &= -i\theta(\tau - \tau') \\ &\times \begin{pmatrix} \sum_i e^{-i(\epsilon_i^0 - ev_g)(\tau - \tau')} & 0 \\ 0 & \sum_i e^{i(\epsilon_i^0 - ev_g)(\tau - \tau')} \end{pmatrix}. \end{aligned} \quad (5)$$

Using the standard NGF technique,¹⁹⁻²¹ the needed Green's functions are obtained as

$$\begin{aligned} G_{11}^r(\epsilon) &= \left[g_{11}^{r-1}(\epsilon) + \frac{i}{2}\Gamma_L + \frac{i|\epsilon|}{2\sqrt{\epsilon^2 - \Delta^2}}\Gamma_R \right. \\ &\quad \left. + \frac{\Delta^2}{4(\epsilon^2 - \Delta^2)} \left(g_{22}^{r-1}(\epsilon) + \frac{i}{2}\Gamma_L + \frac{i|\epsilon|}{2\sqrt{\epsilon^2 - \Delta^2}}\Gamma_R \right) \right]^{-1}, \\ G_{12}^r(\epsilon) &= G_{11}^r(\epsilon) \frac{\Delta}{2\sqrt{\epsilon^2 - \Delta^2}}\Gamma_R \\ &\quad \times \left[g_{22}^{r-1}(\epsilon) + \frac{i}{2}\Gamma_L + \frac{i|\epsilon|}{2\sqrt{\epsilon^2 - \Delta^2}}\Gamma_R \right]^{-1}, \end{aligned} \quad (6)$$

where $\Gamma_{L,R}$ are the appropriate linewidth functions describing the coupling of the CNT to the respective leads. Under the wide-bandwidth approximation, the linewidth functions are independent on the energy variable. This means that the transporting electrons in the leads are equally coupled to different energy levels of CNT. Furthermore, the linewidth functions are set as $\Gamma_L = \Gamma_R = \Gamma$ with small values compared with the energy-level spacing for the symmetric and weak-coupling case. Here G_{11} and G_{12} are the retarded Green's functions of the CNT, which include the proper self-energy of the leads.¹⁹⁻²¹ Then the current and probability of the Andreev reflection are given by

$$I_A = \frac{2e}{h} \int d\epsilon [f_L(\epsilon + ev_L) - f_L(\epsilon - ev_L)] T_A(\epsilon), \quad (7)$$

$$T_A(\epsilon) = \Gamma_L^2 |G_{12}^r(\epsilon)|^2, \quad (8)$$

where f_L denote the Fermi functions of the left lead. Clearly, the conventional tunneling is completely forbidden for $V < \Delta$, and only the Andreev reflection exists. In the following numerical calculations, we discuss in detail the Andreev reflection at zero temperature in the case of $V < \Delta$. We set (1) the temperature $T=0$, (2) the voltage of the right lead $v_R=0$ due to the gauge invariance, and carry out all calculations in units of $h=e=1$. The energy gap of the superconductor is fixed as $\Delta=1.45$ meV (about $5.27 \times 10^{-4}\gamma_0$), corresponding to the Nb leads. The conductance G and the Andreev reflection current I_A are scaled by $G_0=2e^2/h$ and $I_0=2e\gamma_0/h$, respectively.

In order to clearly show the impurity effects on the Andreev reflection current. The current versus gate voltage for (6,6) armchair nanotubes coupled to normal and superconducting leads are plotted in Fig. 1. The nanotube length L has a great influence on the energy structure and the transport properties of the nanotube. Finite-size effects in carbon nanotubes lead to the quantization of the energy levels. The

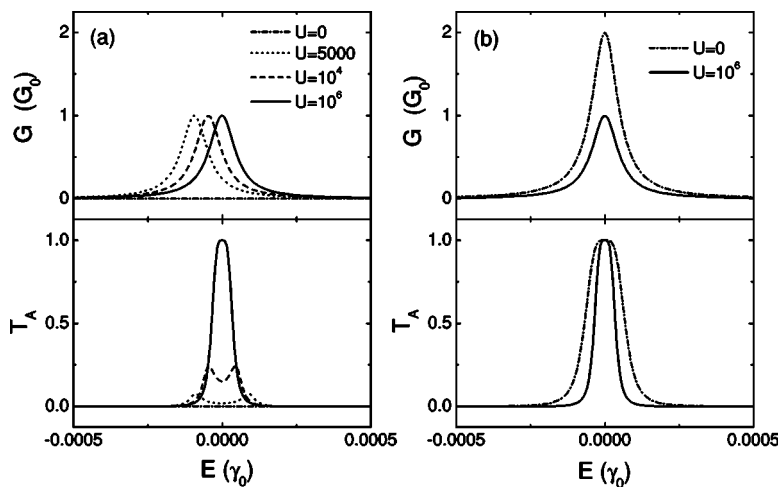


FIG. 2. Conductance G (upper) and Andreev reflection probability T_A (lower) for the (6,6) nanotube of length (a) $L=6$ and (b) $L=7$ with different impurity strength U . Here, $\Gamma=0.1\Delta$.

current peaks are reflections of the band structures of the finite-sized nanotubes, because these resonant states are close to the eigenvalues for small coupling Γ . In the π -electron tight-binding model, the defect-free nanotubes have complete electron-hole symmetry with their Fermi levels at zero.⁷ At $U=0$, the current peaks are symmetric around the Fermi level $E_F=0$. Compared with I_A for $L=6$ and 7, it is evident that positions of the current peaks depend on the nanotube length. There is one peak at the Fermi level for $L=7$, which is absent for $L=6$. This is attributed to the electronic properties of the nanotubes. The band structure of armchair nanotubes consists of two nondegenerate bands that cross the Fermi level at $k_F=2\pi/3a$, with lattice constant a . In finite-length nanotubes, the wave vectors k turn out to be discrete numbers. If there are M cells along the helical line of nanotubes, the quantum box boundary condition leads to $e^{ik(M-1)a}=1$, and then $k=2j\pi/(M-1)a$ with $j=0,1,\dots$. For the armchair nanotube with $M=3N+1$, k_F is an allowed value and the energy gap is zero.²⁶ In general, one resonant peak appears at the Fermi level with $L=3N+1$ (N denoting the number of carbon repeat units), because k_F is now an allowed wave vector, a large conductance exists due to a crossing of two resonant states at the Fermi level.²⁷ For other lengths, k_F is not an allowed wave vector and no resonant state exists at the Fermi level, thus conductance is much smaller due to the energy gap between the resonant states. These are referred to as on-resonance and off-resonance behavior of Andreev reflection, respectively.

The impurity can greatly change the electronic structure of the nanotubes and then the transport properties. In general, the impurity increases the normal reflection.¹⁰ However, it is quite different for finite-sized carbon nanotubes. A new resonant state appears when the incoming electron energies match that of the quasibound state induced by the impurity. For $L=6$ and $L=7$, the impurity with $U=3$ leads to one new peak below the Fermi level as shown in Fig. 1. The resonant states for the conduction and valence bands are quite different due to the impurity, because the electron-hole symmetry is broken by the impurity.⁸ Thus the positions of the current peaks are not symmetric around the Fermi level. The impurity with negative strength $U=-5$ has similar effects on the Andreev reflection current, except that it induces one resonant state above the Fermi level. The resonant state associ-

ated with positive or negative U is analogous to the acceptor or donor state in semiconductors.¹¹ Furthermore, the original peak at the Fermi level for $L=7$ splits into two ones, one of which is still at the Fermi level. The reason is that the single impurity breaks the mirror symmetry planes containing the tube axis, and then the two resonant states at the Fermi level split into two ones. For the vacancy with very large $U=10^6$, the current peaks become symmetric around the Fermi level again, because the position of the resonant state caused by the impurity approaches to the Fermi level at very strong U .¹⁰ For the off-resonant nanotube, the vacancy causes the appearance of a resonance state at the Fermi level, where it is originally zero for the perfect nanotube with $U=0$. For the on-resonant nanotube, the vacancy also induces a new resonant peak at the Fermi energy, and the original one at the Fermi level splits into two ones near the Fermi level. The electron-hole symmetry is recovered at infinitely large U .

To better understand the impurity effects on the Andreev reflections probability, the Andreev reflection probability T_A of the N/CNT/S system and the conductance G of the N/CNT/N system are calculated. The upper plot of Fig. 2(a) shows the conductance G for the (6,6) armchair nanotubes of length $L=6$. At $U=0$, the conductance is zero because there is no resonant state at the Fermi level for $L=6$. At $U=5000$, the impurity leads to one new peak below the Fermi level. The positions of the resonant peaks are not symmetric around the Fermi level due to the broken symmetry caused by the impurity. The other resonant states that extend beyond the region $(-\Delta, \Delta)$ are not shown here. With increasing U , the position of the resonant peak caused by the impurity approaches and finally reaches the Fermi level at infinitely large U .¹⁰ The electron-hole symmetry is recovered again. The lower plot of Fig. 2(a) shows the Andreev reflection probability T_A for the (6,6) armchair nanotubes of length $L=6$. Since the chemical potential of the right superconducting lead is $\mu_R=0$, it is lined up with the Fermi level of the nanotube. If there exists the electron-hole symmetry, μ_R is just located in the middle of two symmetric states with energy ϵ_i and $-\epsilon_i$. A hole can propagate back to the state with the energy $-\epsilon_i$ when an electron incident from the left lead has the energy ϵ_i . Then a Cooper pair creates in the right superconducting lead because of Andreev reflection. At $U=0$, the Andreev reflection probability is zero, because there is no

resonant state within the region $(-\Delta, \Delta)$. Since the level spacings of the CNT are much larger than the gap Δ , only when the resonant state is at the Fermi level can there exist distinct Andreev reflections. At $U=5000$, there appears weak Andreev reflection probability with two small peaks which are symmetric around the Fermi level. The positions of the left peaks of T_A at $U=5000$ and 10^4 are the same with the corresponding ones of G , respectively. The reason is that although the resonant states are not symmetric around the Fermi level, it has a broadened width extended over the Fermi level. Thus it is possible for the Andreev reflections to appear and then the probability is not zero. With increasing U , T_A increases and finally reaches 1 at infinitely large U due to the recover of the electron-hole symmetry. Although the resonant peak in the N/CNT/S system at $U=10^6$ is similar to that in the normal N/CNT/N system, it is different from the conventional resonant tunneling, because the conventional tunneling is completely forbidden for $|E| < \Delta$. In fact, the peak comes from the Andreev reflection.

The conductance for $L=7$ is shown in the upper of Fig. 2(b). At $U=0$, the conductance is two units of quantum conductance $2G_0$, because there are two resonant states that overlap at the Fermi level. At $U=10^6$, G reduces to one unit G_0 , because the original peak with the magnitude $2G_0$ splits due to the perturbation of the impurity, and then there exists only one resonant state at the Fermi level. The curves for G at other impurity strengths U are almost the same with that for $U=10^6$ and not shown here. The lower plot of Fig. 2(b) shows the Andreev reflection probability T_A for $L=7$. At $U=0$, there is a large T_A approaching 1 at the Fermi level due to the existence of two resonant states. At $U=10^6$, the impurity does not reduce the magnitude of the Andreev reflection probability, because there still exists one resonant state at the Fermi level. However, the distribution of T_A with energy is narrowed by the impurity, because only one resonant state contributes to the Andreev reflection. For other impurity strength U , the curves for the T_A are almost the same with that for $U=10^6$ and not shown here.

Figure 3 shows the Andreev reflection current as a function of the bias voltage. For the (6,6) nanotube of length $L=6$, the Andreev reflection current is zero at $U=0$, which shows the off-resonance behavior. While at $U=5000$, the nonzero current appears due to the nonzero Andreev reflection probability. The amplitude of the current increases with increasing U and finally reaches a constant. The reason is that T_A increases and approaches a constant with increasing U . However, the Andreev reflection current is nonzero even

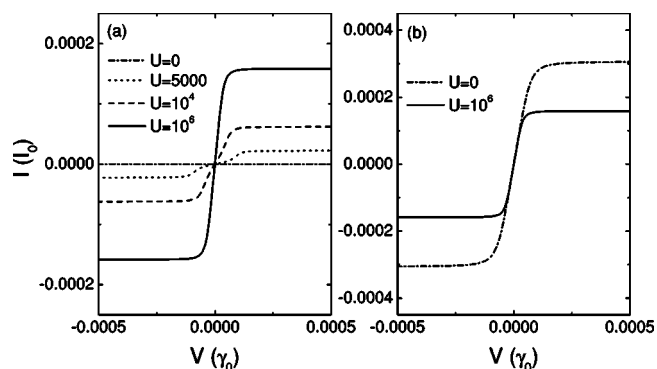


FIG. 3. Andreev reflection current I_A vs the voltage for the (6,6) nanotube of length (a) $L=6$ and (b) $L=7$ with different impurity strength U . Here, $\Gamma=0.1\Delta$.

at $U=0$ for the nanotube with $L=7$, which shows the on-resonance behavior. If there is an impurity in the nanotube, the current is suppressed and the amplitude of the current decreases to about one half of the original one, because only one resonant state contributes to the Andreev reflection. The current still exists even when the impurity strength $U \rightarrow \infty$ because of the existence of one resonant state at the Fermi level. It means that whether the impurity increases or decreases, the Andreev reflection current depends on the nanotube length. The reasons are related to the impurity effect on the Andreev probability T_A as mentioned above.

In summary, the probability and the current of the Andreev reflection for the N/CNT/S hybrid system are studied in detail. The dependence of the Andreev reflection current on the gate voltage shows that the impurity can break the electron-hole symmetry in the nanotubes and the symmetry broken depends distinctly on the impurity strength. The Andreev reflection exhibits the on-resonance and off-resonance behavior at the Fermi level for the nanotubes with length $L=3N+1$ and other lengths, respectively. With increasing the impurity strength, the position of the resonant state induced by it approaches the Fermi level. For the on-resonance case, the impurity narrows the distribution of the Andreev reflection probability and decreases the amplitude of the current. While for the off-resonance case, the impurity enhances the Andreev reflection probability and increases the amplitude of the current.

This project is supported by NSFC under Grant Nos. 90103027 and 50025206, and by the National “973” Projects Foundation of China (No. 2002CB613505).

¹R. Saito, G. Dresselhaus, and M. S. Dresselhaus, *Physical Properties of Carbon Nanotubes* (Imperial College Press, London, 1998).

²J. W. Mintmire, B. I. Dunlap, and C. T. White, *Phys. Rev. Lett.* **68**, 631 (1992).

³N. Hamada, S. I. Sawada, and A. Oshiyama, *Phys. Rev. Lett.* **68**, 1579 (1992).

⁴R. Saito, M. Fujita, G. Dresselhaus, and M. S. Dresselhaus, *Appl. Phys. Lett.* **60**, 2204 (1992).

⁵M. Bochrath, W. Liang, D. Bozovic, J. H. Hafner, C. H. Lieber, M. Tinkham, and H. Park, *Science* **291**, 283 (2001).

⁶L. Chico, L. X. Benedict, S. G. Louie, and M. L. Cohen, *Phys. Rev. B* **54**, 2600 (1996).

⁷L. Chico, V. H. Crespi, L. X. Benedict, S. G. Louie, and M. L.

- Cohen, Phys. Rev. Lett. **76**, 971 (1996).
- ⁸L. Chico, M. P. L. Sancho, and M. C. Muñoz, Phys. Rev. Lett. **81**, 1278 (1998).
- ⁹M. P. Anantram and T. R. Govindan, Phys. Rev. B **58**, 4882 (1998).
- ¹⁰T. Kostyrko, M. Bartkowiak, and G. D. Mahan, Phys. Rev. B **59**, 3241 (1999); **60**, 10 735 (1999).
- ¹¹H. J. Choi, J. Ihm, S. G. Louie, and M. L. Cohen, Phys. Rev. Lett. **84**, 2917 (2000).
- ¹²K. Tsukagoshi, B. W. Alphenaar, and H. Ago, Nature (London) **401**, 572 (1999).
- ¹³A. Yu. Kasumov, R. Deblock, M. Kociak, B. Reulet, H. Bouchiat, I. I. Khodos, Yu. B. Gorbatov, V. T. Volkov, C. Journet, and M. Burghard, Science **284**, 1508 (1999).
- ¹⁴A. F. Morpurgo, J. Kong, C. M. Marcus, and H. Dai, Science **286**, 263 (1999).
- ¹⁵M. R. Graber, T. Nussbaumer, W. Belzig, and C. Schonenberger, cond-mat/0403431 (unpublished).
- ¹⁶Y. Wei, J. Wang, H. Guo, H. Mehrez, and C. Roland, Phys. Rev. B **63**, 195412 (2001).
- ¹⁷J. Jiang, L. Yang, J. Dong, and D. Y. Xing, Phys. Rev. B **68**, 054519 (2003).
- ¹⁸H. K. Zhao, Phys. Lett. A **310**, 207 (2003).
- ¹⁹A. L. Yeyati, A. Martin-Rodero, and J. C. Cruvas, Phys. Rev. B **54**, 7366 (1996).
- ²⁰A. L. Yeyati, J. C. Cuevas, A. Lopee-Davalos, and A. Martin-Rodero, Phys. Rev. B **55**, R6137 (1999).
- ²¹Q. F. Sun, J. Wang, and T. H. Lin, Phys. Rev. B **59**, 3831 (1999).
- ²²M. B. Nardelli, Phys. Rev. B **60**, 7828 (1999).
- ²³M. B. Nardelli and J. Bernholc, Phys. Rev. B **60**, R16 338 (1999).
- ²⁴R. Egger and A. O. Gogolin, Phys. Rev. Lett. **79**, 5082 (1997).
- ²⁵C. Kane, L. Balents, and M. P. A. Fisher, Phys. Rev. Lett. **79**, 5086 (1997).
- ²⁶J. Jiang, J. Dong, and D. Y. Xing, Phys. Rev. B **65**, 245418 (2003).
- ²⁷D. Orlikowski, H. Mehrez, J. Taylor, H. Guo, J. Wang, and C. Roland, Phys. Rev. B **63**, 155412 (2001).